Published online 6 March 2013 *Nucleic Acids Research, 2013, Vol. 41, No. 7* ***4049–4064***
doi:10.1093/nar/gkt127

MAZ-binding G4-decoy with locked nucleic acid and twisted intercalating nucleic acid modifications suppresses *KRAS* in pancreatic cancer cells and delays tumor growth in mice

Susanna Cogoi[1], Sonia Zorzet[2], Valentina Rapozzi[1], Imrich Géci[3], Erik B. Pedersen[3] and Luigi E. Xodo[1,*]

[1]Department of Medical and Biological Sciences, School of Medicine, P.le Kolbe 4, 33100 Udine, Italy, [2]Department of Life Science, University of Trieste, Via Giorgieri 7-9, 34100 Trieste, Italy and [3]Nucleic Acid Center, Institute of Physics, Chemistry and Pharmacy University of Southern Denmark, DK-5230 Odense M, Denmark

Received July 19, 2012; Revised February 5, 2013; Accepted February 10, 2013

ABSTRACT

***KRAS* mutations are primary genetic lesions leading to pancreatic cancer. The promoter of human *KRAS* contains a nuclease-hypersensitive element (NHE) that can fold in G4-DNA structures binding to nuclear proteins, including MAZ (myc-associated zinc-finger). Here, we report that MAZ activates *KRAS* transcription. To knockdown oncogenic *KRAS* in pancreatic cancer cells, we designed oligonucleotides that mimic one of the G-quadruplexes formed by NHE (G4-decoys). To increase their nuclease resistance, two locked nucleic acid (LNA) modifications were introduced at the 3′-end, whereas to enhance the folding and stability, two polycyclic aromatic hydrocarbon units (TINA or AMANY) were inserted internally, to cap the quadruplex. The most active G4-decoy (2998), which had two *para*-TINAs, strongly suppressed *KRAS* expression in Panc-1 cells. It also repressed their metabolic activity (IC_{50} = 520 nM), and it inhibited cell growth and colony formation by activating apoptosis. We finally injected 2998 and control oligonucleotides 5153, 5154 (2 nmol/mouse) intratumorally in SCID mice bearing a Panc-1 xenograft. After three treatments, 2998 reduced tumor xenograft growth by 64% compared with control and increased the Kaplan–Meier median survival time by 70%. Together, our data show that MAZ-specific G4-decoys mimicking a *KRAS* quadruplex are promising for pancreatic cancer therapy.**

INTRODUCTION

A large body of data obtained during the past 20 years shows that the double helix is not the only structure formed by DNA under physiological conditions. DNA is also able to assume alternative structures, in particular within sequences rich in guanine (1). One unusual structure consisting in quartets of guanines stacked on each other, called G-quadruplex or G4-DNA, has drawn the attention of several researchers, and an increasing number of studies indicate that G4-DNA acts as a transcription regulator for certain genes (2–16). A number of studies have been devoted to the human telomeric repeat $(TTAGGG)_n$: the 3′-overhang sequence of the chromosome ends forming G4-DNA structures that stabilize the chromosome against endogenous nucleases and represent a target for anticancer drugs (17–20).

Recent bioinformatic analyses have revealed that G-rich quadruplex-forming sequences occur with a high frequency in genome regions immediately upstream of the transcription start site. This raises the hypothesis that G4-DNA may be involved in transcription regulation (21–24). The seminal study of Hurley and co-workers (3) on c-*MYC* provided the first piece of evidence supporting the role of G4-DNA in transcription, and this stimulated many other investigators to explore functions and properties of G4-DNA. Against this background, our laboratory has focused on the genes of the ras family, in particular *KRAS* and *HRAS*, as their mutant alleles are involved in the pathogenesis of different types of cancers, and their promoters contain G-rich elements potentially capable to fold in G4-DNA (4–7).

The promoter of the human *KRAS* gene contains a nuclease-hypersensitive element (NHE), which is essential for transcription (25–27). Previous studies from our group

*To whom correspondence should be addressed. Tel: +39 0432 494395; Fax: +39 0432 494301; Email: luigi.xodo@uniud.it

have shown that in the presence of potassium, the purine strand of NHE is able to fold into different G4-DNA structures recognized by several nuclear proteins, including hnRNP A1 and PARP-1 (4,5,7,10). We also found that murine analog of NHE binds to MAZ (myc-associated zinc-finger), a zinc-finger factor that activates transcription (8). We, therefore, hypothesized a decoy strategy to inhibit oncogenic *KRAS* in human pancreatic cancer cells. Our approach is based on the rationale that the introduction in the cells of short DNA fragments harboring the binding site of a transcription factor should compete with the binding of the transcription factor to its natural target in the promoter, with the effect of inhibiting transcription. When a decoy strategy was applied against NF-kB and STAT3, the oligonucleotides strongly inhibited the binding of NF-kB or STAT3 to the corresponding *cis*-elements (28–31).

In this study, we have hypothesized that oligonucleotides mimicking *KRAS* quadruplexes should sequester essential proteins and block transcription. To enhance their activity, the anti-*KRAS* decoy oligonucleotides should maintain the 3D structure recognized by the cognate transcription factor and be resistant to the nucleases. We, therefore, designed decoy oligonucleotide variants with terminal locked nucleic acid modifications and polycyclic aromatic hydrocarbon (PAH) insertions such as *para*-TINA (***P***) (*R*)-3-((4-(1-pyrenylethynyl)-benzyl)oxy) propane-1,2-diol (32), *ortho*-TINA (***O***) (*R*)-3-((2-(1-pyrenylethynyl)benzyl)oxy) propane-1,2-diol (33) and AMANY (***Y***) (*S*)-4-(4-(1H-phenanthro[9,10-*d*]imidazol-2-yl)phenoxy)butane-1,2-diol (33). Moreover, we synthesized decoys where one or two loops were replaced with a MADS (***M***) linker (see later in the text). A previous study by Pedersen and co-workers (34) demonstrated that *para*-TINA stabilizes Hoogsteen-type parallel triplexes and exhibited an excellent discrimination between single- and double-stranded DNA. Later, we demonstrated that ***P***, placed at the top of a G4-DNA, brought about a strong stabilization of the structure (10).

In an attempt to design G-quadruplexes with chemical modifications to be used as decoy molecules against the *KRAS* gene, we investigated the impact of PAHs on the folding, stability and potency of the designed oligonucleotides. We found that a G4-decoy with two *para* TINA insertions and two LNA modifications at the 3′-end (2998) strongly inhibited *KRAS* expression, cell growth and colony formation in pancreatic cancer cells. Moreover, 2998 delivered intratumorally in SCID mice bearing a Panc-1 tumor xenograft strongly delayed tumor growth and increased the median survival time compared with mice untreated or treated with control oligonucleotides.

MATERIALS AND METHODS

Oligonucleotides

All unmodified oligonucleotides and dual-labeled polymerase chain reaction (PCR) probes have been purchased from Microsynth (Balgach, Switzerland). The modified oligonucleotides were synthesized on a G-locked nucleic acid (LNA) support as described in Supplementary Data. Their molecular weight was confirmed by MALDI-TOF analysis on an Ultraflex II TOF/TOF system from Bruker (a MALDI-LIFT system) with HPA-matrix (10 mg of 3-hydroxypicolinic acid in 50 mM ammonium citrate/70% acetonitrile) (Table 1). The purities of the final oligonucleotides were found to be >85% by analytical ion-exchange chromatography with a Merck Hitachi LaChrom system on a GenPak-Fax column (Waters).

Circular dichroism

Circular dichroism (CD) spectra have been collected with a JASCO J600 spectropolarimeter equipped with a thermostatted cell holder. Oligonucleotides (3 or 6 μM) have been dissolved in 50 mM Tris–HCl, pH 7.4, 100 mM KCl, and the spectra have been recorded in 0.2- or 0.5-cm quartz cuvette, at increasing temperatures. The ordinate is expressed in millidegrees.

Cell culture, transfection and proliferation assay

Human pancreatic cancer cells (Panc-1) were maintained in exponential growth in Dulbecco's modified Eagle's medium (DMEM) containing 100 U/ml of penicillin, 100 mg/ml of streptomycin, 20 mM L-glutamine and 10% fetal bovine serum (Euroclone, Milano, Italy). Before oligonucleotide transfection, the cells were maintained for 48 h in DMEM with 0.25% fetal bovine serum, then they were plated and transfected by using jetPEI (Polyplus Transfection, Illkirch, France) according to the manufacturer's *in vitro* protocol for DNA oligonucleotides transfection with N/P = 3 (N = nitrogen residues in the jetPEI, P = phosphate groups in the DNA). Transfection of plasmids pCMV-MAZ and pCDNA-3 (control vector) was performed by plating 10^5 cells in each well of a 24-well plate. After 24 h, the cells were transfected with 500 ng of plasmid by using JetPEI (N/P = 5). Panc-1 cells (4×10^4 in each well of a 24-well plate) were transfected with 6 μl of MAZ-specific siRNA (10 μM) (sc-38035 Santa Cruz) or control siRNA (sc-44230, Santa Cruz) with Metafectene SI (Biontex Laboratories GmbH, Martinsried, DE, USA) following the manufacturer's instructions.

The metabolic activity (MA) of Panc-1 cells was measured by plating on a 96-well plate, with 4000 cells in each well, and transfecting them with 72 pmol of oligonucleotide and jetPEI (N/P = 3). MA was measured after 24, 48 or 72 h by a resazurin assay: 25 μM resazurin was added to the cell medium, and the fluorescence was measured after 1 h (Ex 535 nm; Em 590 nm) with a spectrofluorometer EnSpire 2300 Multilabel Reader (Perkin Elmer).

Recombinant MAZ, nuclear extracts and electrophoretic mobility shift assays

The preparation of recombinant MAZ and nuclear extracts was carried out as described in Supplementary Data.

Protein–DNA interactions were analyzed by electrophoretic mobility shift assays (EMSA). Radiolabeled

Table 1. Sequence and composition of the designed G4-decoys

Name	Sequence (5′ → 3′)	PAH insertion	3′-end
32R-3n	GCGGTGTGGGAAGAGGGAAGAGGGGGAGGCAG		
5762	GCGGTGTGGGAAGAGGGAAGAGGGGGAGGCAG		2 LNA
2998	GCGGTGTGGG**P**AAGAGGGAAGA**P**GGGGGAGGCAG	2 *para*-TINA	2 LNA
5763	GCGGTGTGGGAAG**P**AGGGAAGA**P**GGGGGAGGCAG	2 *para*-TINA	2 LNA
5764	GCGGTGTGG**P**GAAGAGGGAAGA**P**GGGGGAGGCAG	2 *para*-TINA	2 LNA
5765	GCGGTGTGGA**P**AAGAGGGAAGA**P**GGGGGAGGCAG	2 *para*-TINA	2 LNA
3014	GCGGTGTGGG**O**AAGAGGGAAGA**O**GGGGGAGGCAG	2 *ortho*-TINA	2 LNA
3044	GCGGTGTGGG**Y**AAGAGGGAAGA**Y**GGGGGAGGCAG	2 *AMANY*	2 LNA
3015	GCGGTGTGGG**P**AAGAGGG**M**GGGGGAGGCAG	1 TINA/1 MADS	2 LNA
3043	GCGGTGTGGG**M**GGGAAGA**P**GGGGGAGGCAG	1 MADS/1 TINA	2 LNA
3069	GCGGTGTGGG**M**GG**M**GGGGGAGGCAG	2 MADS	2 LNA
5153	GCGGTGTCGC**P**AAGACGCAAGACGCGGAGGCAG	1 *para*-TINA	
5154	GCGGTGTCGC**P**AAGACGCAAGACGCGGAGGCCG	1 *para*-TINA	2 LNA

P = *para*-TINA; O = *ortho*-TINA; Y = AMANY; M = MADS.
Underlined nucleotides are LNA modified.

quadruplex 32R-3n (8 or 10 nM) was incubated with 4 µg of MAZ protein or 3 µg of nuclear extract, as indicated in figure captions, for 30 min at room temperature in 20 mM Tris–HCl, pH 8, 30 mM KCl, 1.5 nM $MgCl_2$, 1 mM DTT, 8% glycerol, 1% Phosphatase Inhibitor Cocktail I (Sigma), 5 mM NaF, 1 mM Na_3VO_4 and 2.5 ng/µl of poly [dI-dC] (binding buffer). The analyses were carried out in 5% polyacrylamide gels in 1× Tris–borate (TB) at 20°C.

Western blot assays

A total of 2.25×10^5 Panc-1 cells were transfected with 595 pmol of decoys (350 nM); cells were collected in sodium dodecyl sulfate (SDS) buffer (4% SDS, 20% glycerol and 0.125 M Tris–HCl, pH6.8), and proteins were quantified. Equal amounts of proteins were separated by 10% SDS–polyacrylamide gel electrophoresis (PAGE) and blotted for 2 h at 70 V in 25 mM Tris, 192 mM glycine and 20% methanol at 4°C on a nitrocellulose membrane. The membranes were incubated with a primary anti-*KRAS* antibody (diluted 1:250) (Abcam, ab102007) and a secondary rabbit IgG peroxidase-conjugated antibody (1:10.000) (Calbiochem). The β-actin level in each sample was measured with anti–β-actin antibody (1:10.000, CP01, Calbiochem) and a mouse IgM peroxidase-conjugated antibody (1:10.000) (Calbiochem). The antibodies were diluted in 10 mM Tris, pH 7.9, 150 mM NaCl, 0.05% Tween and 5% bovine serum albumin. The signal was developed with Super-Signal West Pico or Femto (Pierce) and detected with ChemiDOC XRS, Quantity One 4.6.5 software (Bio-Rad Laboratories, CA, USA).

RNA extraction and real-time PCR

RNA extraction was performed as described in Supplementary Data. Real-time PCR multiplex reactions were performed with 1× Kapa Probe fast qPCR kit for KRAS and housekeeping genes hypoxanthine–guanine phosphoribosyltransferase (HPRT) and β2-microglobulin, 200 nM of each primer, 100 nM of each probe and ~0.7 µl of reverse transcription. The PCR cycle was 3 min at 95°C, 50 cycles 10 s at 95°C and 60 s at 58°C. MAZ reactions were performed with 1× Kapa SYBR fast qPCR kit, 300 nM of each primer, 0.7 µl of reverse transcription reaction. Primers are hmaz forward 5′-CTCCAGTCCC GCTTCT and hmaz reverse 5′-GGGAGCAAGTCCAC CT. The PCR cycle was 3 min at 95°C, 40 cycles of 10 s at 95°C and 30 s at 58°C. PCR reactions were performed with a CFX 96 real-time PCR controlled by Bio-Rad CFX Manager V1.5 (Bio-Rad Laboratories, CA, USA). All expressions were normalized with housekeeping genes. The sequences of the primers and probes used for the amplifications are as follows: for *KRAS*, the probe is FAM-TAC TCCTCTTGACCTGCTGTG-BHQ1 (accession No. NM_033360, from 352 to 372), the sense primer is 5′-C GAATATGATCCAACAATAGAG (from 271 to 292, NM_033360) and the antisense primer is 5′-ATGTACT GGTCCCTCATT (from 379 to 396, NM_033360). For β2-microglobulin, the probe is ROX-TATGCCTGCCG TGTGAACC-BHQ2 (from 352 to 370, NM_004048), the sense primer is 5′-CCCCACTGAAAAAGATGA (from 333 to 350 NM_004048) and the antisense primer is 5′-CCATGATGCTGCTTACAT (from 415 to 432, NM_004048). For HPRT1, the probe is Cy5-CTTGCG ACCTTGACCATCTT-BHQ2 (from 633 to 652, NM_000194), the sense primer is 5′-CTTGATTGTGGA AGATATAATTG (from 557 to 575, NM_000194) and the antisense primer is 5′-TATATCCAACACTTCGTG G (from 672 to 690, NM_000194).

Apoptosis assays

Caspase activity assay was performed with Apo-ONE™ Homogeneous Caspase-3/7 Assay (Promega), according to the manufacturer's protocol. Annexin V–propidium iodide assay was performed with Annexin V Apoptosis Detection Kit (Santa Cruz), following the manufacturer's instructions. Cell cycle analysis was carried out in the cells (2.5×10^4) treated with 360 pmol oligonucleotide. The cells have been harvested 24 h after oligonucleotide transfection and treated for 1 h at 4°C with a solution containing 70% ethanol and 30% phosphate-buffered saline (PBS). The cells were then washed with PBS and stained with propidium iodide (50 ng/µl) in the presence of RNase

A (100 ng/μl) in PBS for 1 h. Flow cytometry measurements were performed with FACScan (Becton Dickinson).

Colony-forming assay

Panc-1 cells were transfected with the G4-decoys as described earlier in the text for proliferation assays. After 18 h, the wells were treated with trypsin, and one-third of the volume of each well was seeded on 100-mm diameter plates and grown under normal culture conditions. After 1 week, the cells were stained with 2.5% methylene blue in 50% ethanol for 10 min. Colonies of >50 cells were counted.

Double-filter DNA–protein binding assay

This assay was performed as described previously (35). A concise description is provided in Supplementary Data.

Human tumor xenograft model in SCID mice

SCID mice of ~20 g were implanted subcutaneously with human Panc-1 cells (15×10^6 cells) in 100 μl of physiological solution using a 23-gauge needle. Each mouse received one injection in the right flank for the development of a tumor xenograft in 6–7 weeks. Treatment with decoy and control oligonucleotides started when the tumor had a size between 30 and 50 mm^3 corresponding to 30–50 mg. The mice were randomized in groups of four animals and injected intratumorally with a solution containing 2 nmol oligonucleotide, *in vivo*-jetPEI (Polyplus Tranfection) at N/P ratio 6 and 5% glucose. Each mouse, except those of the untreated group, received three doses of oligonucleotides at Days 1, 6 and 11. The tumor growth was measured with a caliper twice a week. Tumor volume was calculated according to $V = [(\text{small diameter})^2 \times (\text{large diameter})]\pi/6$ every 4 days up to 44 days since the first treatment. The tumor volume (cm^3) was transformed in mass (mg), assuming a density of 1. All procedures involving animals have been approved (N. 42) by the Ethical Committee of the University of Trieste.

The data were statistically analyzed and subjected to factorial ANOVAs. Statistical significance level was set at $P < 0.05$. When the individual effect of the treatments and the interactions between the independent variables in a 2×2 ANOVA were significant, a *post hoc* Tukey–Kramer test for significance of the differences in the mean values was performed. For all analyses, we used the Systat package (SYSTAT Inc., Evanston, IL, USA). For survival analyses, we obtained the Kaplan–Meier curves (SPSS 11); the P values were calculated by a logrank test.

RESULTS

MAZ binds to G4-DNA of the *KRAS* promoter and activates transcription

The promoter of the human *KRAS* oncogene contains an NHE, which is essential for transcription (25–27). NHE is composed of six runs of guanines (G-runs 1–6 from the 5′-end) separated by 'AAGA', 'TGT', 'A' and 'C' and exhibits a complex structural polymorphism. Within the purine strand of NHE, we identified three quadruplex-forming motifs, namely, 32R, 21R and 32R-3n, each forming a stable G-quadruplex (4,5,7,10) (Figure 1 A and B). We proposed for each quadruplex a putative structure deduced from DMS-footprinting and CD data (4,5,7,10). We previously had found by chromatin immunoprecipitation that MAZ, a transcription factor recognizing blocks of guanines, whose consensus sequence is GGG(A/C)GG (36), binds to the murine analog of NHE (8). As the murine and human NHE sequences show a high homology, MAZ should also bind to human NHE, which contains two MAZ-binding sites, G GGCGG and GGGAGG, respectively, at the 5′- and 3′-ends (Figure 1C). Mobility shift experiments showed that recombinant MAZ (Supplementary Figure S1) recognizes all three G4-DNA structures of NHE, in particular the one formed by 32R-3n with which it forms a retarded band of high intensity (Figure 2A). The radiolabeled *KRAS* quadruplexes were also incubated with nuclear extracts from pancreatic (Panc-1) and cervical (HeLa) cancer cells. It can be seen that with both extracts, the three *KRAS* quadruplexes form at least two DNA–protein complexes, in keeping with the fact that several proteins were pulled down by the purine strand of NHE in the folded conformation (5).

To explore the functional role played by MAZ within the KRAS transcription, we measured *KRAS* mRNA in Panc-1 cells where the MAZ gene was either silenced with siRNA or overexpressed with pCMV-MAZ. The results showed that when MAZ was overexpressed, *KRAS* transcription was 3.5-fold upregulated compared with the control (cells treated with a non-specific plasmid) (Figure 2B). In contrast, when MAZ was silenced (residual MAZ was 10% of control), *KRAS* transcription was downregulated to 40% of the control (Figure 2C). Together, the data suggest that MAZ is a transcription factor that activates human *KRAS* transcription. This is consistent with previous data from our laboratory showing that MAZ activates the murine *KRAS* gene (8).

A decoy strategy to inhibit *KRAS* in pancreatic cancer cells

Hingorani and co-workers (37) have demonstrated that the expression of mutant *KRAS* in mouse pancreas is sufficient to initiate cancer. *KRAS* encodes for a GTP-binding protein that activates the MAPK/ERK pathway controlling cell proliferation. When protein $p21^{RAS}$ is mutated, it loses its capacity to hydrolyze GTP to GDP, thus remaining locked into an active state that stimulates constitutively cell growth. Increasing evidence supports the notion that *KRAS* is a key element in the pathogenesis of several types of cancer and a primary target for anticancer drugs. *KRAS* is mutated in >90% of pancreatic adenocarcinomas and in ~50% of colorectal carcinomas (38–40).

In the light of our findings, we hypothesized that the expression of *KRAS* in pancreatic cancer cells can be downregulated by using decoy oligonucleotides mimicking one of the potential NHE quadruplexes. The G4-decoys

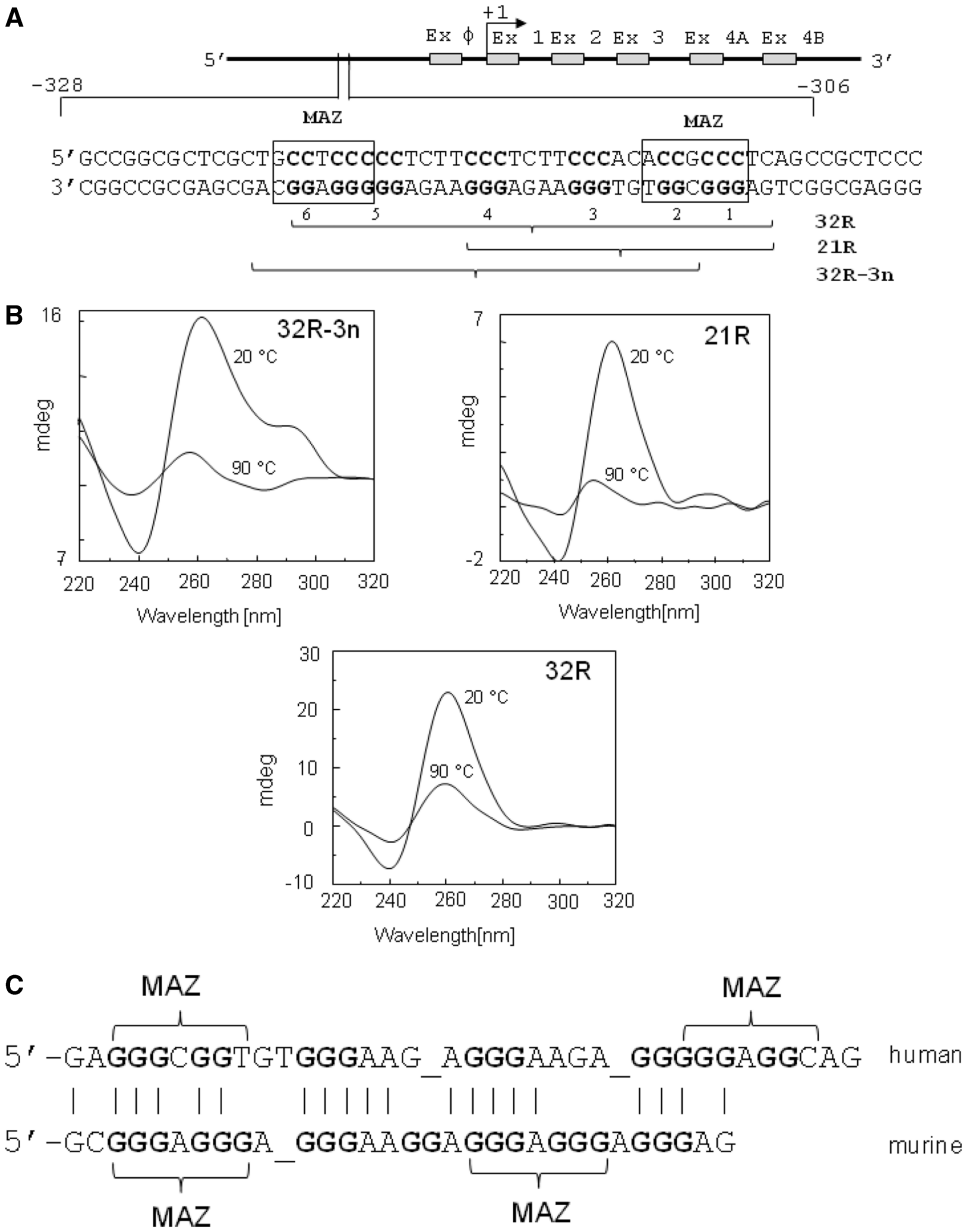

Figure 1. (**A**) Sequence of the NHE present in the human *KRAS* promoter upstream of the transcription start site. NHE contains six guanine repeats and three quadruplex-forming motifs, named 32R (repeats 1–6), 32R-3n (repeats 2–6) and 21R (repeats 1–4); (**B**) CD of the quadruplex-forming sequences at 20°C and 90°C; (**C**) sequence homology between human and murine NHEs. Human NHE contains two binding sites [(GGG(A/C)GG] for the transcription factor MAZ at the 5′- and 3′-ends.

given to the cells should compete with the binding of MAZ to the *KRAS* promoter, inhibit *KRAS* expression and, given the mitogenic character of the gene, also cell growth (6,10).

To sort out which NHE quadruplex the G4-decoys should mimic, we transfected Panc-1 cells with oligonucleotides 32R, 32R-3n and 21R (100, 200, 400, 800 and 1200 nM) in the presence of jetPEI as a transfection reagent (Polyplus, Transfection) and measured by a resazurin assay the MA of the cells 48 h after treatment. We found that oligonucleotide 32R-3n caused the strongest inhibition of the MA, with an IC_{50} of 700 ± 49 nM (data not shown). We, therefore, focused our study on the quadruplex-forming motif 32R-3n.

The affinity between quadruplex 32R-3n and recombinant MAZ was assessed by a double-filter–binding assay, as previously described (35) (Figure 2D). We incubated the radiolabeled 32R-3n quadruplex (5 nM, 100% in the folded conformation) for 1 h at room temperature with increasing amounts of MAZ in a buffer added with 2 μg/μl of poly d(I-C) (unspecific competitor). As a control, quadruplex 32R-3n was incubated with increasing amounts of two unspecific proteins: trypsinogen and ovalbumin. The percentage of quadruplex bound to MAZ was plotted as a function of protein concentration, and the curve was best-fitted to a standard binding equation (Sigma Plot 10). A K_D of 320 ± 2 nM was obtained. The K_D of recombinant MAZ for quadruplex 32R-3n

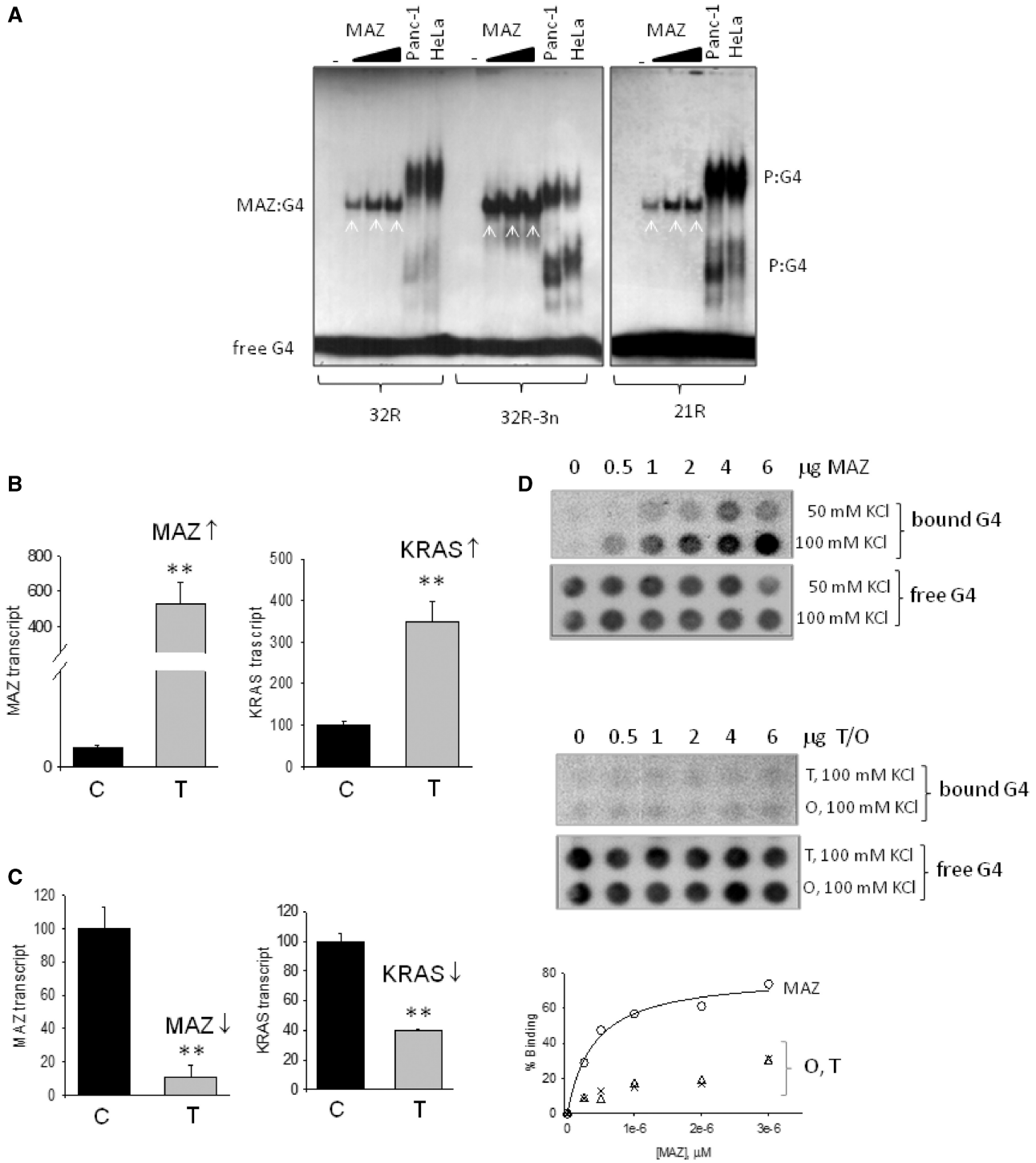

Figure 2. (**A**) Mobility shift assay showing the binding of recombinant MAZ to *KRAS* quadruplexes of NHE. Increasing amounts of MAZ (1, 2 and 4 µg) were incubated for 30 min in binding buffer with 10 nM radiolabeled G-quadruplex and run in 5% PAGE in TB buffer (500 V, 3 h, 20°C). The white arrows indicate the MAZ-G4 complexes. The radiolabeled quadruplexes have also been incubated with nuclear extract from Panc-1 and HeLa cells (3 µg). They form two main G4-protein complexes (P:G4). Bovine serum albumin (4 µg) was used as a control. (**B**) Left panel shows the level of MAZ mRNA in Panc-1 cells transfected with pCMV-MAZ; right panel shows *KRAS* mRNA level in the same cells. C = cells treated with an empty plasmid, T = treated cells. (**C**) Left panel shows the level of MAZ mRNA in Panc-1 cells in which MAZ was silenced with siRNA; right panel shows *KRAS* mRNA level in the same cells. C = cells treated with control siRNA, T = treated cells. Student's *t*-test, $^{**}P < 0.01$. (**D**) Filter-binding assay showing the binding of recombinant MAZ to quadruplex 32R-3n, in 50 and 100 mM KCl. Top membrane (nitrocellulose) shows MAZ [or control proteins, trypsinogen (T), ovalbumin (O)] bound to the quadruplex; bottom membrane (nylon+) shows unbound radiolabeled quadruplex. The fraction of quadruplex 32R-3n bound to MAZ is plotted against the MAZ concentration. The binding curve relative to MAZ was best-fitted to a standard binding equation. A K_D of 320 ± 2 nM was obtained.

seemed to not be different from the K_Ds reported for the binding of other recombinant proteins (nucleolin, nucleophosmin and hRNP A1) to G4-DNA, but it was one order of magnitude higher than the K_D relative to the binding of cellular Sp1 to c-Kit quadruplex (41–44).

The quadruplex-forming motif 32R-3n was used to design transcription factor G4-decoys specific for *KRAS*.

Design of anti-KRAS G4-DNA decoys with chemical insertions

A critical issue about the use of decoy molecules is their stability in the serum and cellular environment. Indeed, when oligonucleotides with a natural sugar–phosphate backbone, as 32R-3n or TINA-modified analogs, are incubated in serum, they are degraded in few hours. We, therefore, introduced at the 3′-end of the G4-decoys two LNA modifications to make them resistant against the nucleases (Supplementary Figure S2). In addition, we increased their thermostability by introducing between G10-A11 and A21-G22 the following PAH insertions (10) (Figure 3): *para*-TINA (***P***) in decoy 2998; *ortho*-TINA (***O***) in decoy 3014; AMANY (***Y***) in decoy 3044. We designed decoys also with (i) ***P*** and MADS (***M***), a phenylen-bis-naphthalene linker replacing either the first (decoy 3015) or the second (decoy 3043) 'AAGA' loop and (ii) two ***M*** linkers replacing both loops (decoy 3069). As a control, we designed two oligonucleotides with five G → C mutations that prevent them from folding into a quadruplex: the first with one ***P*** unit (5153), the second with both ***P*** and LNA modifications (5154) (Table 1).

PAGE shows that ***P*** and ***O*** insertions promote the intramolecular folding of 32R-3n (Figure 4A). Indeed, after an overnight incubation in 100 mM KCl, although 32R-3n migrates as a mixture of mono and bimolecular quadruplexes, its *para*- or *ortho*-TINA analogs (2998 and 3014) migrate only as a folded species, but characterized by different CD spectra, with ellipticity $R_{290/265}$ ratios of 0.83 and 1.3, respectively (Figure 4B). In contrast, compound 3044 with ***Y*** insertions migrated about half as folded and half as multimolecular G4-DNA species, mostly in the antiparallel conformation ($R_{290/265}$ = 1.52). When one lateral loop of 2998 was replaced with ***M*** (3015 or 3043), the resulting oligonucleotides migrated as mono- and multi-molecular species. Instead, when both loops were replaced with ***M*** (3069), the sequence migrated as bi- and multi-molecular parallel (*p*) quadruplexes ($R_{290/265}$ = 0.3).

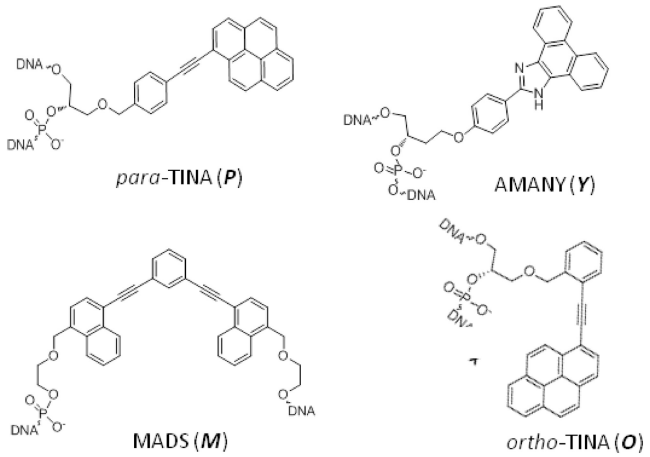

Figure 3. Chemical insertions introduced in the quadruplex-forming sequence 32R-3n. The primary structures of the designed G4-decoys are reported in Table 1.

The active G4-DNA decoys compete with the binding of MAZ to NHE

As a first screening aimed to find out which of the designed G4-decoys was biologically active, we measured their capacity to lower the MA in Panc-1 cells. The cells were treated with 600 nM G4-decoys in the presence of jetPEI, and after an incubation of 48 h, a resazurin assay was performed. The compound that mostly reduced the MA (~70% compared with control) was 2998 with ***P***/LNA modifications. Sequence 3014 with ***O***/LNA and unmodified 32R-3n caused a weaker decrease of the MA (~50%). Instead, a modest effect on the MA (<40%) was observed with all the other modified sequences (3044, 3015, 3043 and 3069), as well as control oligonucleotides 5153 and 5154 (Figure 4C). We then asked whether there is any relationship between CD/PAGE data and the biological activity. The following observations can be made: (i) the most active sequences are those folding into a monomolecular quadruplex (2998 and 3014) whose CD shows two positive peaks at 265 and 290 nm and a negative peak at 240 nm, typical of a mixed *p*/*ap* quadruplex topology (45); (ii) the sequences forming a quadruplex with one or two loops replaced by ***M*** (3015, 3043 and 3069) exhibit low activity; and (iii) the sequences (3044 and 3043) folding into a quadruplex presumably in the *ap* conformation ($R_{290/265} > 2.9$) also show low activity.

According to our hypothesis, the active decoys should mimic the quadruplex formed by 32R-3n and sequester the transcription factor MAZ. We, therefore, determined their affinity for MAZ by a PAGE competition assay (Figure 4D). It can be seen that 2998 and 3014 strongly compete with the binding of MAZ to quadruplex 32R-3n. A 10-fold excess reduces the binding, but a 50-fold excess completely eliminates it. A similar result was obtained with unmodified 32R-3n and 3044. Oligonucleotide 3044 behaved in a somewhat surprising manner because it competed with the binding of MAZ to 32R-3n without showing any impact on the MA in Panc-1 cells. As we will argue further on, this might be due to the fact that 3044 aggregates in the cell medium (Supplementary Figure S2). Control oligonucleotides 5153 and 5154 did not compete with the binding of MAZ to quadruplex 32R-3n because of their being unstructured. Interestingly, the oligonucleotides 3043, 3015 and 3069, lacking either one or two loops, were also unable to bind to MAZ, suggesting the importance of the loops in the MAZ–quadruplex interaction.

To further investigate the activity of the designed decoys, we focused on the most active compound 2998 and the least active 3044, as well as on control sequences 5153 and 5154.

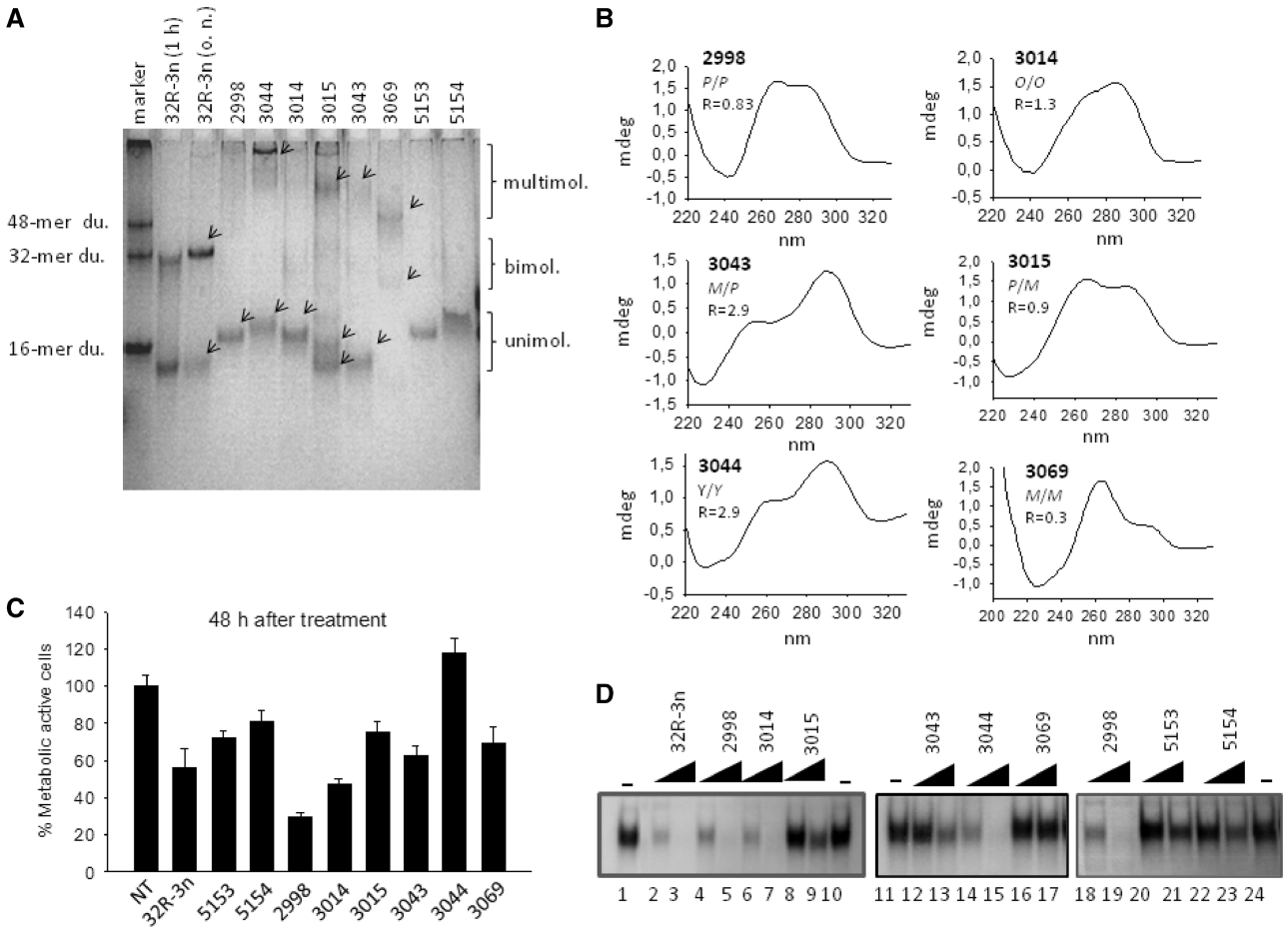

Figure 4. (**A**) Twenty per cent PAGE in TB, pH 8, 50 mM KCl, 20°C (200 V, 8 h) of the designed G4-decoys (5 μM), including the control sequences 5153 and 5154. Before loading, the oligonucleotides have been incubated overnight in the buffer containing 100 mM KCl. The 32R-3n was loaded after 1 h or overnight incubation. (**B**) CD spectra in 50 mM Tris–HCl, pH 7.4, 100 mM KCl, 2-mm cuvette, of the designed G4-decoys at 20°C. ***P*** = para-TINA; ***O*** = ortho-TINA, ***Y*** = AMANY, ***M*** = MADS. R is the CD ratio between the signals at 290 over 265 nm. (**C**) Percentage of MA compared with control (NT) of Panc-1 cells treated with 600 nM G4-decoys and control oligonucleotides, carried out 48 h after oligonucleotide treatment. NT = non-treated cells. (**D**) EMSA showing the capacity of the designed decoys to compete the binding of MAZ to quadruplex 32R-3n. All lanes contained 8 nM radiolabeled 32R-3n and 4 μg of recombinant MAZ. Lanes 1, 10, 11 and 24 show the DNA–protein complex in the absence of a decoy competitor. The other lanes show that the DNA–protein complex is competed by the decoys, 10- and 50-fold in excess to radiolabeled 32R-3n. Analysis: 5% PAGE in TB, 500 V, 3 h, 20°C. Before being used, the competitor decoys and probe 32R-3n were annealed in 100 mM KCl.

Putative structure of the lead G4-decoy 2998 containing two *para*-TINA insertions

Sequence 32R-3n exists as a monomer ↔ dimer equilibrium and shows a CD with ellipticities at 265 and 290 nm, in 100 mM KCl (Figures 1B and 4A) (Supplementary Figure S3). When the 'GCGG' repeat at the 5′-end is cut-off or replaced with 'GCAA', 32R-3n forms only a dimeric quadruplex, whose CD is characterized by a 265 nm ellipticity (Figure 5A and B). We, therefore, attributed the 290 nm ellipticity to the monomeric quadruplex formed by 32R-3n. The intramolecular quadruplex showing ellipticities at 265 and 290 nm is that with a mixed *p*/*ap* folded topology.

The DMS-footprinting of the monomolecular form of 32R-3n, obtained at 10 nM, shows that guanines G4, G8–G10, G15–G17, G22–G26 are protected from DMS methylation in 100 mM KCl: a typical signature of quadruplex formation (Supplementary Figure S4). The methylation pattern is reported in Figure 5A. As the first 'GCGG' repeat is interrupted by a cytosine, 32R-3n should fold into a quadruplex where one base is looped out from the G-tetrad core [the nuclear magnetic resonance of a quadruplex with a bulged topology has been recently reported (46,47)]. The fact that the G22–G26 repeat is protected from DMS suggests that 32R-3n should form more than one conformer, by involving G22–G23–G24, G23–G24–G25 and G24–G25–G26. However, a TMPyP4-photocleavage assay of quadruplex 32R-3n revealed a strong reactivity of G22. As TMPyP4 stacks on the G-tetrads besides binding to the loops (48,49), the G22–G23–G24 conformer is probably more abundant (Supplementary Figure S4).

When two ***P*** insertions were introduced in 32R-3n, adjacent to a guanine repeat, i.e. between G10–A11 and A21–G22, the modified strand (2998) showed a dramatic increase of the T_M from 50°C to 79°C, in 100 mM KCl.

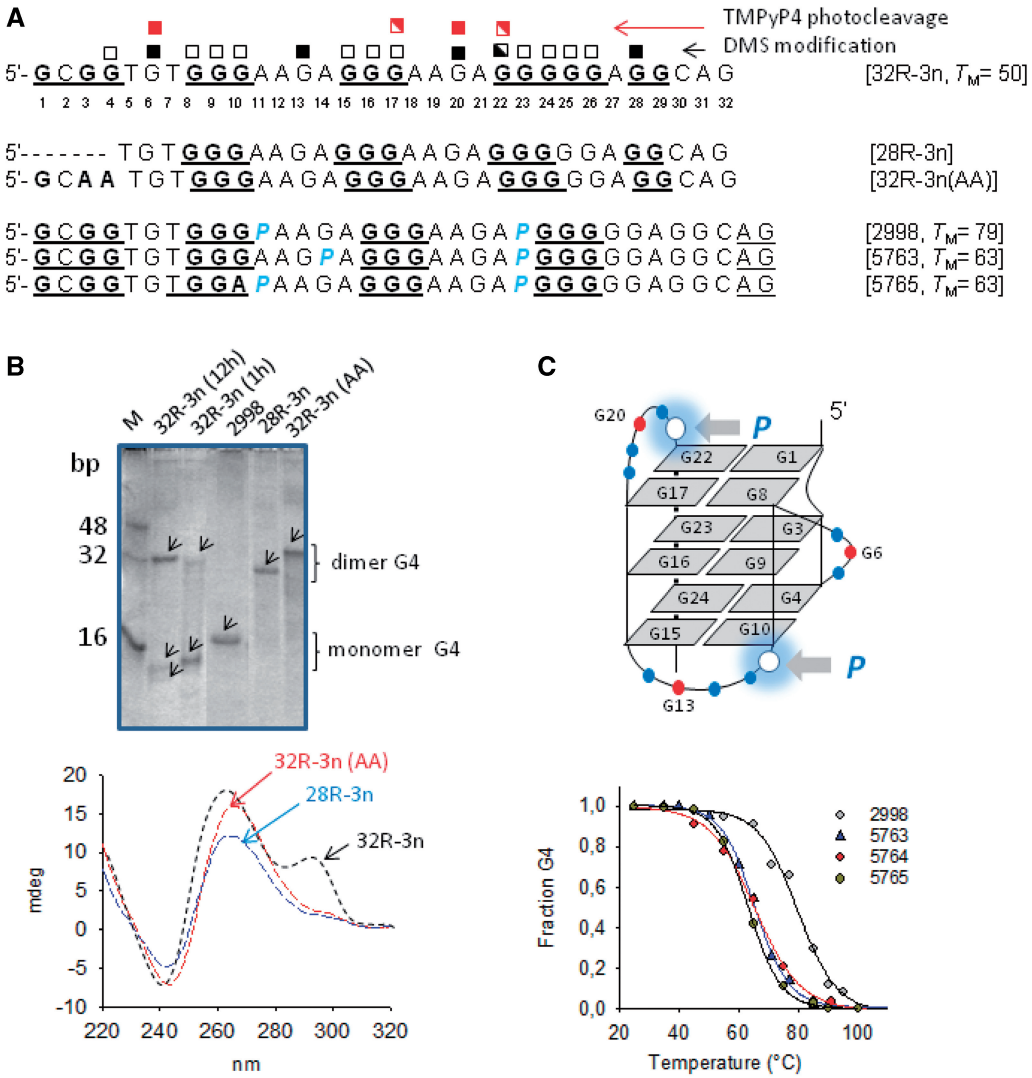

Figure 5. (**A**) The 32R-3n sequence showing the bases methylated by DMS (black square, methylated; white square, protected from methylation) and photocleaved by TMPyP4/light (red square). Sequence variants of 32R-3n and decoy 2998 are also shown. (**B**) Eighteen per cent PAGE in the presence of 50 mM KCl (200 V, 8 h, 20°C); CD of 5 μM oligonucleotides in 100 mM KCl. (**C**) Putative mixed *p*/*ap* structure of 2998; CD-melting curves of 2998 and decoy variants. All experiments performed in 50 mM Tris–HCl, pH 7.4 and 100 mM KCl.

This suggests that the pyrene chromophores stack on the external G-tetrads, thus stabilizing the quadruplex. As 2998 migrates with one sharp band and shows a CD with two ellipticities at 265 and 290 nm ($R_{290/265}$ = 0.83), it should assume a mixed *p*/*ap* conformation (Figure 5C). To corroborate the proposed structure, we synthesized a sequence variant where ***P*** between G10 and A11 was shifted inside the loop (5763). Expectedly, the T_M of the resulting quadruplex dropped to 63°C because one ***P*** stacking was lost. In the same way, when we disrupted the guanine repeat G8–G10, either by replacing G10 with A (5765) or by shifting ***P*** next to G9 (5764), the T_M dropped to 63°C and 64°C, respectively, because the two variants could form only two G-tetrad quadruplexes (PAGE and CD spectra of these decoy variants are reported in Supplementary Figure S5).

Taken together, the data suggest that 2998 should form a highly stable mixed *p*/*ap* quadruplex with two *para*-TINA insertions stacking on the external G-tetrads.

G4-decoy with *para*-TINA insertions represses *KRAS*

The level of *KRAS* mRNA in Panc-1 cells treated with 600 nM 2998, 32R-3n, 3044 and controls 5153, 5154, was determined by quantitative real-time PCR (Figure 6A). The amount of *KRAS* transcript was referred to the housekeeping genes *HPRT* and β2-microglobulin. It can be seen that 24 h after treatment, *KRAS* mRNA in the cells treated with 32R-3n and 2998 was reduced to 20 and 10%, respectively, of the control (untreated cells). In contrast, the cells treated with decoys 3044, 5143 and 5154 showed *KRAS* mRNA expression levels similar to that of the untreated cells. This result correlates nicely with the inhibition of the MA caused by the oligonucleotides. Next, we measured by a western blot analysis the level of the KRAS protein in the treated Panc-1 cells, to rule out the possibility that the observed mRNA repression was the result of a temporary fluctuation unable to effectively impact on translation. As the half-life of human $p21^{RAS}$ proteins has been found to vary

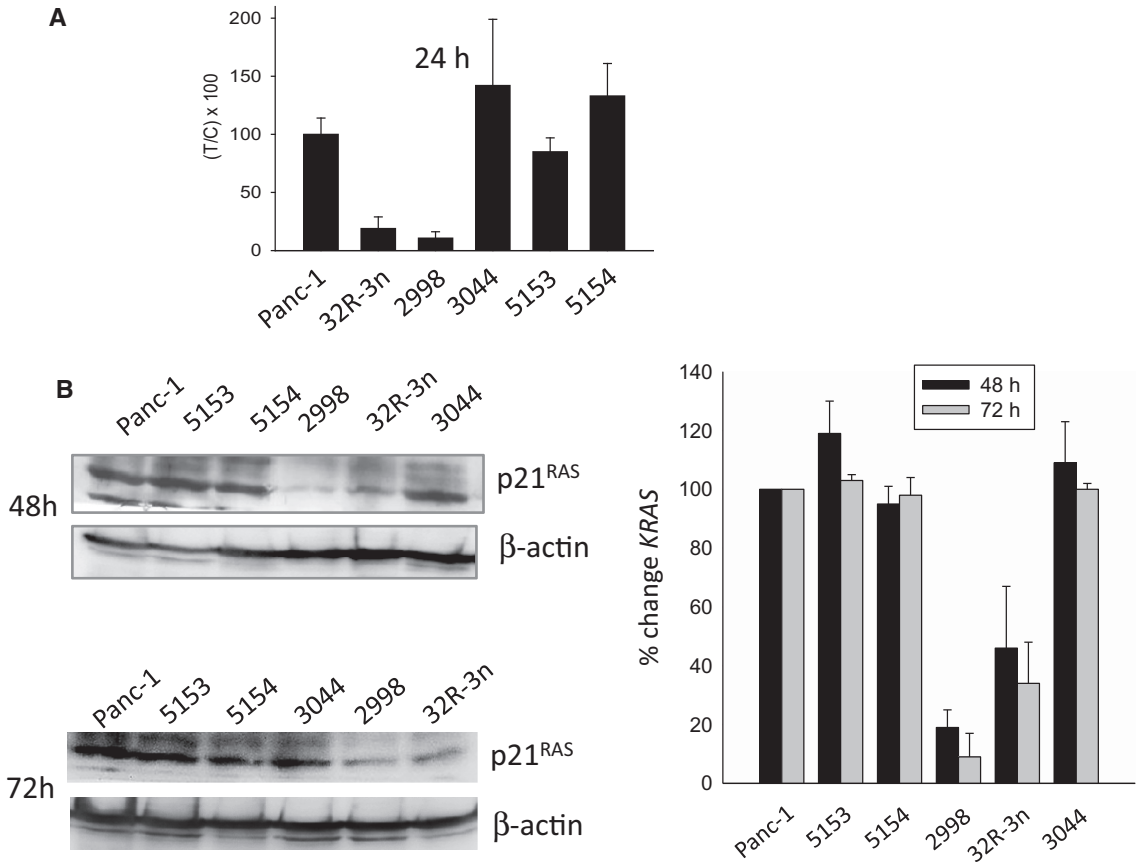

Figure 6. (**A**) Level of *KRAS* mRNA in Panc-1 cells treated with 600 nM G4-decoy and control oligonucleotides, measured 24 h after decoy transfection in the presence of jetPEI. *KRAS* mRNA was measured with respect to housekeeping genes β2-microglobulin and HPRT. Ordinate reports the percentage of *KRAS* transcript, i.e T/C × 100 where T is (*KRAS* transcript)/(β2-microglobulin and HPRT transcripts) in the decoy-treated cells, whereas C is (*KRAS* transcript)/(β2-microglobulin and HPRT transcripts) in the decoy-untreated cells. (**B**) Western blot showing the level of $p21^{RAS}$ at 48 and 72 h in Panc-1 cells after transfection with decoy and control oligonucleotides, in the presence of jetPEI. The data have been normalized to β-actin. The band intensities have been measured with ChemiDOC XRS apparatus (BioRad). Right panel shows a histogram reporting the average values of three independent western blots (12% SDS–PAGE, 1 h, 180 V).

from 20 (50) to 36 h (51), the western blots were carried out at 48 and 72 h after treatment. Panc-1 cells, 48 and 72 h after transfection with decoys 32R-3n, 2998, 3044, 5153 and 5154, were lysed, and the protein extract was analyzed by immunoblotting with a KRAS-specific antibody. Figure 6B shows the results of a typical experiment. We performed three independent experiments, the average data of which are reported in a histogram. It can be seen that 2998 and 32R-3n suppress protein $p21^{RAS}$ to 19 ± 6 and 46 ± 21% of the control at 48 h and to 9 ± 8 and 34 ± 14% at 72 h after treatments. In accord with the MA and real-time mRNA data, 3044, 5153 and 5154 did not show any activity.

The higher inhibitory activity of 2998 compared with 32R-3n can be rationalized in terms of its stronger capacity to fold into a specific intramolecular quadruplex ($R_{290/265} = 0.9$) and better resistance against the nucleases.

G4-DNA decoy 2998 inhibits the clonogenic capacity of Panc-1 cells

As mutant *KRAS* constitutively stimulates cell growth in Panc-1 cancer cells, a reduced level of protein $p21^{RAS}$ is expected to inhibit cell growth and colony formation in the treated cells (10). To test this hypothesis, Panc-1 cells, treated with G4-decoys 2998, 3044, 32R-3n and control oligonucleotides 5153 and 5154, have been seeded in plates ('Materials and Methods' section). After an incubation of 7 days, the colonies were stained with methylene blue (visible colonies have at least 50 cells) (Figure 7). The data show that untreated cells form colonies that are visible with methylene blue and uniformly distributed in the plate, whereas the cells treated with 2998 form a dramatically lower number of colonies. Instead, 3044, 5153 and 5154 did not produce any significant inhibitory effect on colony formation, thanks to their incapacity to block the MA of the cells and knockout *KRAS*. The colonies were counted, and the results were reported in a histogram. It was found that the percentage of clonogenicity of Panc-1 cells treated with 2998 was reduced to 6 ± 1% of the control, whereas oligonucleotides 3044, 5153 and 5154 showed no inhibitory effect. In comparison, the wild-type 32R-3n reduced the percentage of colonies to 44 ± 6% of the control. This is in keeping with the fact that only a fraction of 32R-3n (<50%) assumes a folded conformation causing a partial downregulation of protein $p21^{RAS}$.

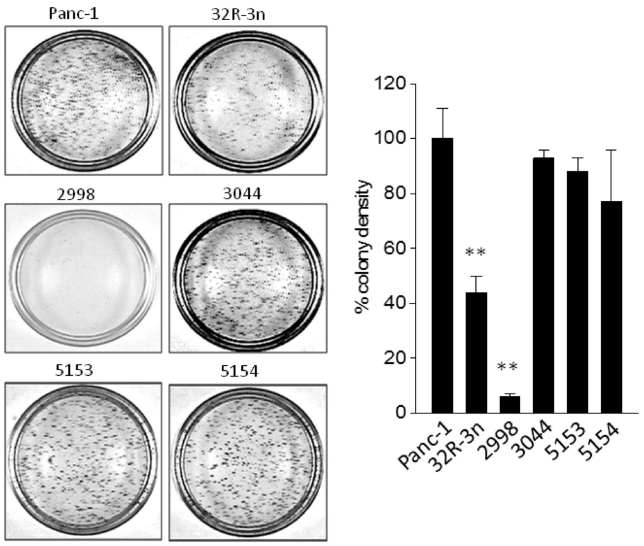

Figure 7. Colony-forming assay in Panc-1 cells treated with decoy and control oligonucleotides (32R-3n, 2998, 3044, 5153 and 5154). Colonies have been fixed and stained with methylene blue, 7 days after cell transfection. The histogram shows the percentage of colony formation of the treated cells compared with untreated cells. Difference from control is supported by Student's t test, $^{**}P < 0.01$.

G4-DNA decoy 2998 induces cell death mediated by apoptosis

Previous studies have shown that the suppression of *KRAS* in cancer cells results in cell growth inhibition mediated by apoptosis (52,53). We, therefore, investigated whether this also occurs in cells treated with the G4-decoys 2998 and 32R-3n. Figure 8A shows that, compared with untreated cells, 2998 and 32R-3n did indeed activate caspases 3/7 in Panc-1 cells, whereas 3044, 5153 and 5154 did not. This finding nicely matches with the data reported earlier in the text. Apoptosis induced by 2998 and 32R-3n was also confirmed by a fluorescence-activated cell sorting (FACS) analysis of the cell cycle, which showed that Panc-1 cells treated with 600 nM decoy 2998 or 32R-3n were indeed characterized by a typical pre-G1 peak indicative of cell debris resulting from apoptosis (31 and 29% of apoptotic cells, respectively), whereas untreated cells or cells treated with decoys 3044, 5153 and 5154 did not show a pre-G1 peak (Figure 8B).

Finally, the presence of apoptotic cells in the treated samples was also determined by propidium iodide–annexin V assay. An early event occurring in apoptosis is the loss of plasma membrane asymmetry. This is because phosphatidylserine flips from the inner to the outer leaflet of the plasma membrane, thus getting exposed to the external cellular environment. To measure this event by flow cytometry, we used fluorescein isothiocyanate labeled annexin V, a protein recognizing phosphatidylserine. To distinguish between early apoptotic cells and late apoptotic (dead) cells, annexin V was used in combination with propidium iodide, which stained the dead cells (Figure 8C). In keeping with caspase 3/7 assay, 2998 and, to a lower extent, 32R-3n promoted apoptosis, whereas 5153 and 5154 did not. The percentages of early and late apoptotic cells induced by the oligonucleotides 2998, 32R-3n, 5153 and 5154 are 36.1 ± 7, 30.5 ± 9, 8.4 ± 4 and 6.8 ± 2, respectively. All data are summarized in Supplementary Table S6.

G4-decoy 2998 reduces tumor growth and increases the median survival time in SCID mice bearing a Panc-1 xenograft

The activity of decoy 2998, which seemed to be strong in cell-based *in vitro* experiments, was also assessed *in vivo*, in SCID mice bearing a Panc-1 tumor xenograft. It should be remembered that the growth of Panc-1 cells strongly depends on *KRAS* expression because this gene is mutated in exon 1; thus, it produces a constitutively active $p21^{RAS}$ protein that stimulates cell growth (37,38). SCID mice bearing a subcutaneous Panc-1 tumor xenograft of ~30–50 mm^3 were randomized into four groups of four mice each. They were intratumorally injected with a 50-µl solution containing 2 nmol oligonucleotide/mouse and *in vivo*-jetPEI. This treatment was repeated three times (at Days 1, 6 and 11), and the tumor size was measured every 4 days with a caliper. Apart from the untreated group (Group 1, treated only with 5% glucose), the other groups were treated with 2998 (Group 2), control oligonucleotides 5153 (Group 3) and 5154 (Group 4), which both are not able to fold into a quadruplex thanks to their five G → C mutations. The data of Figure 9A show that from Day 13 after the first treatment, the G4-decoy 2998 strongly reduced the growth of the tumor xenograft as compared with the non-treated or control-treated groups ($P < 0.001$). Typical images of an untreated and a 2998-treated mice are reported in Supplementary Figure S7. In Figure 9B, we report the Kaplan–Meier survival curves showing that the median survival times of the various groups was Group 1 (untreated) 60.5 days, Group 2 (treated with 2998) 103.5 days, Group 3 (treated with 5153) 71 days and Group 4 (treated with 5154) 71.5 days. The median survival time of the mice treated with 2998 increased by 70% compared with the control groups ($P < 0.006$).

Together, our data indicate that oligonucleotide 2998 is an effective transcription factor G4-decoy that shows *in vitro* a marked capacity to repress *KRAS* and cell growth in Panc-1 cells. Furthermore, *in vivo*, it strongly delays the growth of a Panc-1 xenograft in SCID mice and significantly increased the median survival time of the mice treated with 2998.

DISCUSSION

In this study, we have tested the capacity of chemically modified G4-DNA decoy oligonucleotides to knockout the *KRAS* oncogene in Panc-1 cells—the primary genetic lesion responsible for the malignant transformation of pancreatic cells (38–40)—and to delay *in vivo* the growth of a Panc-1 tumor xenograft in SCID mice. The decoy approach, which has been introduced 2 decades ago, provides a powerful tool to target the genetic roots of a disease. The term decoy is often confounded with

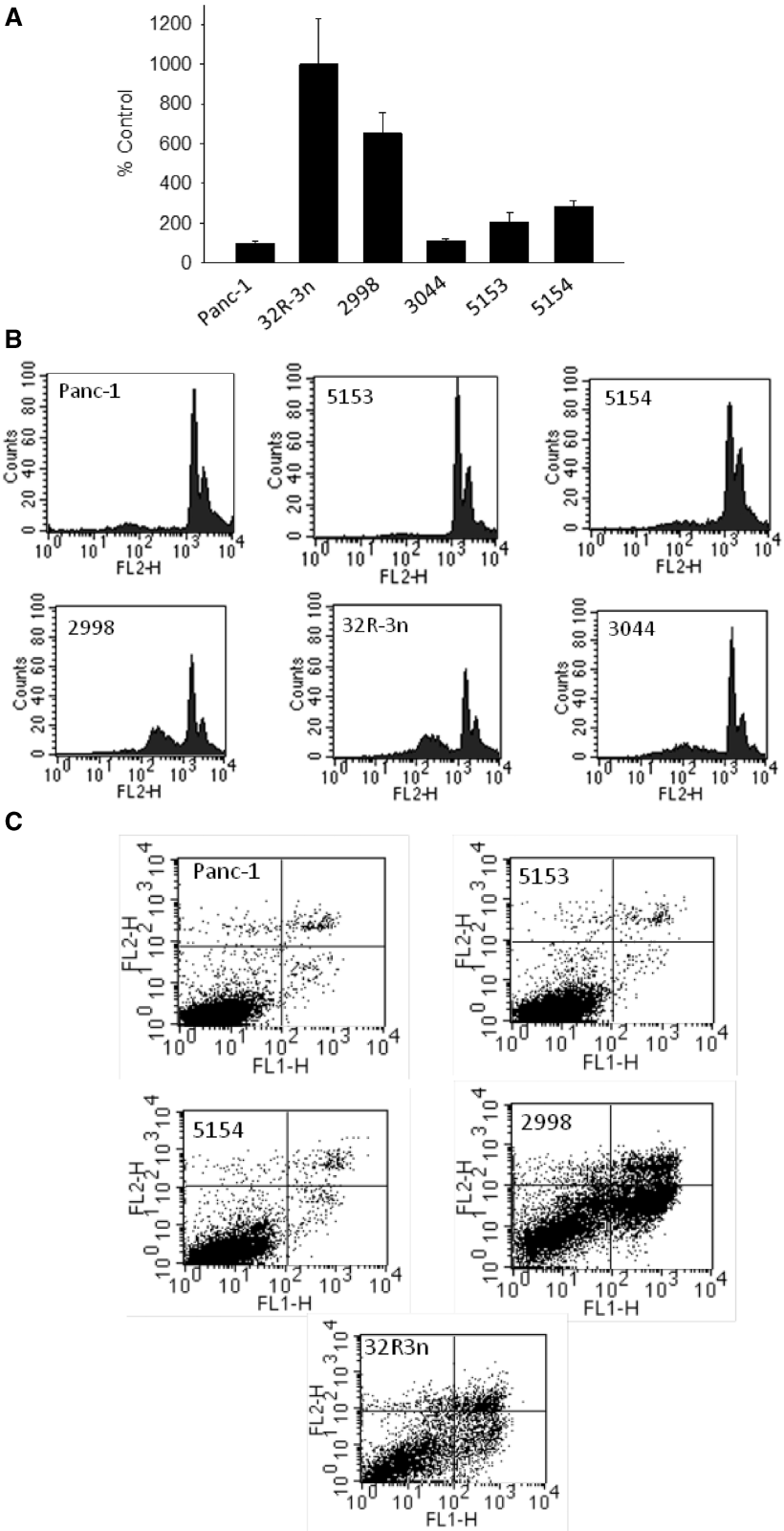

Figure 8. (**A**) Apo ONE assay showing caspase 3/7 activation in Panc-1 cells 30 h after treatment with decoy and control oligonucleotides. (**B**) Cell cycle analysis of Panc-1 cells 24 h after treatment with decoy and control oligonucleotides. The cells were stained with propidium iodide and analyzed by flow cytometry. (**C**) Propidium iodide/annexin V assay for the detection of early and late apoptotic Panc-1 cells, 40 h after transfection with the control and decoy oligonucleotides.

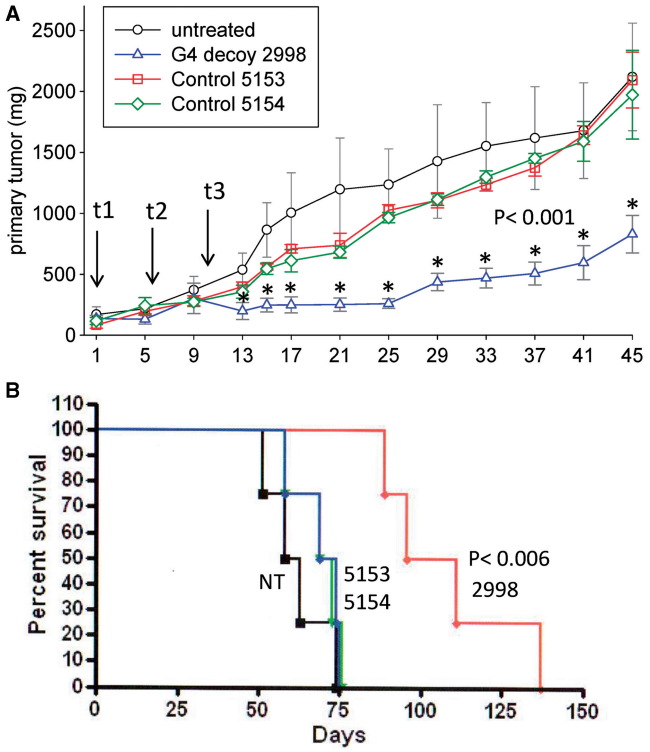

Figure 9. (**A**) Effect of decoy and control oligonucleotides intratumorally injected in SCID mice bearing a subcutaneous Panc-1 xenograft. The ordinate axis reports the growth of the tumor xenograft (mg). The oligonucleotide treatment (2 nmol/mouse) was performed three times at Days 1, 6 and 11 (t1, t2 and t3). From Day 13, the Panc-1 xenograft in the mice group treated with 2998 grew more slowly than in the non-treated mice group or mice groups treated with controls 5153 and 5154 ($P < 0.001$). (**B**) Kaplan–Meier curves showing the effect of decoy 2998 compared with the untreated group or the groups treated with 5153 or 5154. The median survival time of the group treated with 2998 is 103.5 days, statistically higher than the median survival time of the control groups (71 and 71.5 days) ($P < 0.006$).

aptamer, but the two molecules are conceptually different. Aptamers are DNA or RNA oligonucleotides that bind specifically to a given target and are usually obtained from a synthetic combinatorial library by exponential enrichment iterative methodology (SELEX) (54). Instead, decoys are DNA or RNA fragments with a naturally occurring sequence—normally a protein-binding site—which are designed to specifically bind to the target protein. The saturation of the protein-binding site with decoys makes the protein unable to subsequently bind to its target.

DNA decoys are a class of targeted therapeutic agents in rapid expansion. Transcription factor decoy oligonucleotides have been used to modulate gene expression *in vitro* and *in vivo*. Decoys for NF-kB (29,30,55–58), STAT3 (59,60), p53 (61), E2F (62,63) and AP-1(64) have been previously proposed. Our decoys are mimics of a G4-DNA structure that can be formed in NHE of the human *KRAS* promoter. It is known that certain G-rich oligonucleotides show an anti-proliferative activity in several cancer cells (65–67). Although the mechanism of the quadruplex aptamers is not yet clear, evidence that their action is associated to protein binding has already been provided. For instance, nucleolin plays a role in mediating the effect of the well-known quadruplex-forming aptamer AS1411 (68). In the present study, we demonstrate that the designed G4-decoys exhibiting an anti-proliferative effect in pancreatic cancer cells (10) bind to transcription factor MAZ, thus subtracting from the *KRAS* promoter a protein essential for transcription activation.

MAZ was first identified as a GA-box–binding transcription factor in the *c-MYC* promoter that controls transcription initiation and termination (69). Its functional role in the context of transcription is complex because some genes are activated by MAZ (36,70–73), and others are repressed (74,11). Here, we provide evidence that MAZ activates transcription of the human *KRAS* gene. A similar behavior was already observed with murine *KRAS* (8).

To inhibit the *KRAS* oncogene in pancreatic cancer cells, we designed anti-MAZ decoys with the sequence of 32R-3n, but containing two types of chemical modifications: LNA modifications at the 3′-end and PAH insertions at specific positions. LNA nucleotides have an extra connection between the 2′ oxygen and 4′ carbon, thus forming a bridge that 'locks' the ribose in the 3′-*endo* conformation. This makes the quadruplex-forming oligonucleotides resistant against nucleases. Indeed, although quadruplex 32R-3n or 32R-3n with ***P*** insertions is degraded in serum, their analogs with two LNA at the 3′ show a fairly good resistance. Previous studies demonstrated that the introduction of ***P*** at the ends of duplex or quadruplex DNA strongly increases the T_M (10,75). An interesting effect of TINA (***P*** or ***O***) is its capacity to favor an intramolecular folding of the strand in which they have been inserted. Indeed, we found that decoy 2998 with ***P*** and decoy 3014 with ***O*** migrate in a polyacrylamide gel as monomolecular species only, whereas the other decoys with ***Y*** or ***M*** modifications form mono- or multimolecular species. In addition, 3044 with ***Y*** insertions showed a high propensity to aggregate *in vitro*. It is possible that in the crowding intracellular conditions, this decoy aggregates even further, with the result that its decoy potency is severely compromised.

Although the PAH units introduced in sequence 32R-3n enhanced the thermostability of the resulting quadruplex (PAH-containing quadruplexes have $T_M > 70°C$; data not shown), only 2998 with two ***P*** insertions showed strong activity, *in vitro* and *in vivo*. DMS-footprinting, CD and a sequence variant analysis suggest that 2998 should adopt a 3 G-tetrad mixed *p/ap* quadruplex with ***P*** stacked on the external G-tetrads. In a previous work, we proposed for an analog of 2998, devoid of LNA modifications at 3′-end, a mixed p/ap quadruplex with 2 G-tetrads. The apparent incongruence is probably because of the fact that the TINA insertions interfere with DMS-footprinting (10).

The *RAS* family of oncogenes is mutated in ~30% of all human cancers (76). *KRAS* is mutated at codon 12 in ~80% of pancreatic adenocarcinomas, 50% of colorectal carcinomas and 40% of non-small cell lung cancer (38–40). As previous studies have shown that mutant

KRAS is sufficient to initiate cancer in rat pancreas (37), *KRAS* represents an important target for anticancer drugs. Pancreatic cancer cells are dependent on mutant ras functions, and the downregulation of *KRAS* has been demonstrated to affect cell growth (52,77). This notion is supported by previous studies from our laboratories (78) and also comes from a recent study where mutant *KRAS* expression was knocked down by adenovirus-mediated siRNA (52). All these studies demonstrate that the inhibition of activated RAS protein increases apoptosis. The results of the present study are consistent with the aforementioned observations. In particular, we found that *KRAS* suppression mediated by the G4-decoy 2998 strongly decreases cell growth and colony formation of Panc-1 cells. As already found in non-small lung cancer cells, the knockdown of ras in Panc-1 cells promotes apoptosis, as indicated by annexin V and propidium iodide, caspase 3/7 and cell cytometry assays. Our *para*-TINA and LNA-modified G4-decoy 2998 shows a remarkable capacity to slow down the growth of a Panc-1 tumor xenograft in nude mice. After three treatments, tumor growth was completely arrested up to Day 25. At longer time points, the tumor xenograft initiated a steady growth but at a lower rate than the controls did. This suggests that on increasing the number of treatments, it should be possible to arrest completely tumor growth over a longer period. As we expected, control 5153 and 5154 showed an unspecific antitumor effect that vanished at longer time points. This is likely because of the presence of guanines in these oligonucleotides (65,66).

In summary, we have developed an anti-MAZ G4-decoy oligonucleotide with locked nucleic acid and twisted-intercalating nucleic acid modifications that mimics a quadruplex structure formed by a critical *KRAS* G-element. When this engineered oligonucleotide is transferred into the cells, it knocks out *KRAS* by a putative mechanism based on the sequestration of MAZ. Thanks to its chemical modifications, the decoy is rather resistant to the nucleases and produces a strong effect in pancreatic cancer cells, as well as in a tumor xenograft. Caspase 3/7, FACS and annexin V–propidium iodide assays showed that the inhibitory effect promoted by decoy 2998 is mediated by apoptosis. The results of our study suggest that the G4-decoy 2998, engineered with LNA and TINA modifications, may have potential in treating pancreatic cancer or sensitizing tumor cells to chemotherapy.

SUPPLEMENTARY DATA

Supplementary Data are available at NAR Online: Supplementary Materials and Methods, Supplementary Table 1 and Supplementary Figures 1–7.

ACKNOWLEDGEMENTS

Plasmids pGEX-hMAZ and pCMV-MAZ were provided by RIKEN BRC, which is participating in the National Bio-Resources Project of the MEXT. Ms Tanja M. True is gratefully acknowledged for her contribution to oligonucleotide synthesis.

FUNDING

Italian Association for Cancer Research, AIRC [2010 Ref. 10546]; PRIN 2009. Funding for open access charge: AIRC, Italian Association for Cancer Research.

Conflict of interest statement. None declared.

REFERENCES

1. Choi,J. and Majima,T. (2011) Conformational changes of non-B DNA. *Chem. Soc. Rev.*, **40**, 5893–5909.
2. Sen,D. and Gilbert,W. (1988) Formation of parallel four-stranded complexes by guanine-rich motifs in DNA and its implications for meiosis. *Nature*, **334**, 364–366.
3. Siddiqui-Jain,A., Grand,C.L., Bears,D.J. and Hurley,L.H. (2002) Direct evidence for a G-quadruplex in a promoter region and its targeting with a small molecule to repress c-MYC transcription. *Proc. Natl Acad. Sci. USA*, **99**, 11593–11598.
4. Cogoi,S. and Xodo,L.E. (2006) G-quadruplex formation within the promoter of the KRAS proto-oncogene and its effect on transcription. *Nucleic Acids Res.*, **34**, 2536–2549.
5. Cogoi,S., Paramasivam,M., Spolaore,B. and Xodo,L.E. (2008) Structural polymorphism within a regulatory element of the human KRAS promoter: formation of G4-DNA recognized by nuclear proteins. *Nucleic Acids Res.*, **36**, 3765–3780.
6. Membrino,A., Cogoi,S., Pedersen,E.B. and Xodo,L.E. (2011) G4-DNA formation in the HRAS promoter and rational design of decoy oligonucleotides for cancer therapy. *PLoS One*, **6**, e24421.
7. Paramasivam,M., Cogoi,S. and Xodo,L.E. (2011) Primer extension reactions as a tool to uncover folding motifs within complex G-rich sequences: analysis of the human KRAS NHE. *Chem. Commun. (Camb.)*, **47**, 4965–4967.
8. Cogoi,S., Paramasivam,M., Membrino,A., Yokoyama,K.K. and Xodo,L.E. (2010) The KRAS promoter responds to Myc-associated zinc finger and poly(ADP-ribose) polymerase 1 proteins, which recognize a critical quadruplex-forming GA-element. *J. Biol. Chem.*, **285**, 22003–22016.
9. Paramasivam,M., Membrino,A., Cogoi,S., Fukuda,H., Nakagama,H. and Xodo,L.E. (2009) Protein hnRNP A1 and its derivative Up1 unfold quadruplex DNA in the human KRAS promoter: implications for transcription. *Nucleic Acids Res.*, **37**, 2841–2853.
10. Cogoi,S., Paramasivam,M., Filichev,V., Géci,I., Pedersen,E.B. and Xodo,L.E. (2009) Identification of a new G-quadruplex motif in the KRAS promoter and design of pyrene-modified G4-decoys with antiproliferative activity in pancreatic cancer cells. *J. Med. Chem.*, **52**, 564–568.
11. Palumbo,S.L., Memmott,R.M., Uribe,D.J., Krotova-Khan,Y., Hurley,L.H. and Ebbinghaus,S.W. (2008) A novel G-quadruplex-forming GGA repeat region in the c-myb promoter is a critical regulator of promoter activity. *Nucleic Acids Res.*, **36**, 1755–1769.
12. Sun,D., Liu,W.J., Guo,K., Rusche,J.J., Ebbinghaus,S., Gokhale,V. and Hurley,L.H. (2008) The proximal promoter region of the human vascular endothelial growth factor gene has a G-quadruplex structure that can be targeted by G-quadruplex-interactive agents. *Mol. Cancer Ther.*, **7**, 880–889.
13. Qin,Y., Rezler,E.M., Gokhale,V., Sun,D. and Hurley,L.H. (2007) Characterization of the G-quadruplexes in the duplex nuclease hypersensitive element of the PDGF-A promoter and modulation of PDGF-A promoter activity by TMPyP4. *Nucleic Acids Res.*, **35**, 7698–7713.
14. Rankin,S., Reszka,A.P., Huppert,J., Zloh,M., Parkinson,G.N., Todd,A.K., Ladame,S., Balasubramanian,S. and Neidles,S. (2005) Putative DNA quadruplex formation within the human c-kit oncogene. *J. Am. Chem. Soc.*, **127**, 10584–1059.

15. Lew,A., Rutter,W.J. and Kennedy,G.C. (2000) Unusual DNA structure of the diabetes susceptibility locus IDDM2 and its effect on transcription by the insulin promoter factor Pur-1/MAZ. *Proc. Natl Acad. Sci. USA*, **97**, 12508–12512.
16. Brooks,T.A. and Hurley,L.H. (2009) The role of supercoiling in transcriptional control of MYC and its importance in molecular therapeutics. *Nat. Rev. Cancer*, **9**, 849–861.
17. Neidle,S. (2010) Human telomeric G-quadruplex: the current status of telomeric G-quadruplexes as therapeutic targets in human cancer. *FEBS J.*, **277**, 1118–1125.
18. Zhou,X. and Xing,D. (2012) Assays for human telomerase activity: progress and prospects. *Chem. Soc. Rev.*, **41**, 4643–4656.
19. Wu,Y. and Brosh,R.M. (2010) G-quadruplex nucleic acids and human disease. *FEBS J.*, **277**, 3470–3488.
20. Phan,A.T., Kuryavyi,V. and Patel,D.J. (2006) DNA architecture: from G to Z. *Curr. Opin. Struct. Biol.*, **16**, 288–298.
21. Maizels,N. (2006) Dynamic roles for G4 DNA in the biology of eukaryotic cells. *Nat. Struct. Mol. Biol.*, **13**, 1055–1059.
22. Huppert,J.L. and Balasubramanian,S. (2007) G-quadruplexes in promoters throughout the human genome. *Nucleic Acids Res.*, **35**, 406–413.
23. Todd,A.K., Johnston,M. and Neidle,S. (2005) Highly prevalent putative quadruplex sequence motifs in human DNA. *Nucleic Acids Res.*, **33**, 2901–2907.
24. Eddy,J. and Maizels,N. (2006) Gene function correlates with potential for G4 DNA formation in the human genome. *Nucleic Acids Res.*, **34**, 3887–3896.
25. Yamamoto,F. and Perucho,M. (1988) Characterization of the human c-K-ras gene promoter. *Oncogene Res.*, **3**, 125–130.
26. Jordano,J. and Perucho,M. (1986) Chromatin structure of the promoter region of the human c-K-ras gene. *Nucleic Acids Res.*, **14**, 7361–7378.
27. Jordano,J. and Perucho,M. (1988) Initial characterization of a potential transcriptional enhancer for the human c-K-ras gene. *Oncogene*, **2**, 359–366.
28. Govan,J.M., Lively,M.O. and Deiters,A. (2011) Photochemical control of DNA decoy function enables precise regulation of nuclear factor kB activity. *J. Am. Chem. Soc.*, **133**, 13176–13182.
29. De Stefano,D., De Rosa,G. and Carnuccio,R. (2010) NFkappaB decoy oligonucleotides. *Curr. Opin. Mol. Ther.*, **12**, 203–213.
30. Wang,T., Li,Q.H., Hao,G.P. and Zhai,J. (2010) Antitumor activity of decoy oligodeoxy-nucleotides targeted to NF-kappaB in vitro and in vivo. *Asian Pac. J. Cancer Prev.*, **11**, 193–200.
31. Souissi,I., Najjar,I., Ah-Koon,L., Schischmanoff,P.O., Lesage,D., Le Coquil,S., Roger,C., Dusanter-Fourt,I., Varin-Blank,N., Cao,A. *et al.* (2011) STAT3-decoy oligonucleotide induces cell death in a human colorectal carcinoma cell line by blocking nuclear transfer of STAT3 and STAT3-bound NF-κB. *BMC Cell Biol.*, **12**, 12–14.
32. Filichev,V.V., Gaber,H., Olsen,T.R., Jørgensen,P.T., Jessen,C.H. and Pedersen,E.B. (2006) Twisted intercalating nucleic acids—intercalator influence on parallel triplex stabilities. *Eur. J. Org. Chem.*, **17**, 3960–3968.
33. Osman,A.M.A., Jørgensen,P.T., Bomholt,N. and Pedersen,E.B. (2008) Using an aryl phenanthroimidazole moiety as a conjugated flexible intercalator to improve the hybridization efficiency of a triplex-forming oligonucleotide. *Bioorg. Med. Chem.*, **16**, 9937–9947.
34. Filichev,V.V. and Pedersen,E.K. (2005) Stable and selective formation of Hoogsteen-type triplexes and duplexes using twisted intercalating nucleic acids (TINA) prepared via postsynthetic Sonogashira solid-phase coupling reactions. *J. Am. Chem. Soc.*, **127**, 14849–14858.
35. Wong,I. and Lohman,T.M. (1993) A double-filter method for nitrocellulose-filter binding: application to protein-nucleic acid interactions. *Proc. Natl Acad. Sci. USA*, **90**, 5428–5432.
36. Parks,C.L. and Shenk,T. (1996) The serotonin 1a receptor gene contains a TATA-less promoter that responds to MAZ and Sp1. *J. Biol. Chem.*, **23**, 4417–4430.
37. Tuveson,D.A., Shaw,A.T., Willis,N.A., Silver,D.P., Jackson,E.L., Chang,S., Mercer,K.L., Grochow,R., Hock,H., Crowley,D. *et al.* (2004) Endogenous oncogenic K-ras(G12D) stimulates proliferation and widespread neoplastic and developmental defects. *Cancer Cell*, **5**, 375–387.
38. Malumbres,M. and Barbacid,M. (2003) RAS oncogenes: the first 30 years. *Nat. Rev. Cancer*, **3**, 459–465.
39. Yanes,L., Groffen,J. and Valenzuela,D.M. (1987) cKRAS mutations in human carcinomas occur preferentially in codon 12. *Oncogene*, **1**, 315–318.
40. Minamoto,T., Mai,M. and Ronai,Z. (2000) K-ras mutation: early detection in molecular diagnosis and risk assessment in colorectal, pancreas and lung cancers- a review. *Cancer Detect. Prev.*, **24**, 1–12.
41. Gonzales,V., Guo,K., Hurley,L. and Sun,D. (2009) Identification and characterization of nucleolin as a c-myc G-quadruplex-binding protein. *J. Biol. Chem.*, **284**, 23622–23635.
42. Federici,L., Arcovito,A., Scaglione,G.L., Scaloni,F., Lo Sterzo,C., Di Matteo,A., Falini,B., Giardina,B. and Brunori,M. (2010) Nucleophosmin C-terminal leukemia-associated domain interacts with G-rich quadruplex forming DNA. *J. Biol. Chem.*, **285**, 37139–37149.
43. Paramasivam,M., Membrino,A., Cogoi,S., Fukuda,H., Nakagama,H. and Xodo,L.E. (2009) Protein hnRNP A1 and its derivative Up1 unfold quadruplex DNA in the human KRAS promoter: implications for transcription. *Nucleic Acids Res.*, **37**, 2841–2853.
44. Raiber,E.A., Kranaster,R., Lam,E., Nikan,M. and Balasubramanian,S. (2012) A non-canonical DNA structure is a binding motif for the transcription factor SP1 in vitro. *Nucleic Acids Res.*, **40**, 1499–1508.
45. Dai,J., Dexheimer,T.S., Chen,D., Carver,M., Ambrus,A., Jones,R.A. and Yang,D. (2006) An intramolecular G-quadruplex structure with mixed parallel/antiparallel G-strands formed in the human BCL-2 promoter region in solution. *J. Am. Chem. Soc.*, **128**, 1096–1098.
46. Mukundan,V.T., Do,N.Q. and Phan,A.T. (2011) HIV-1 integrase inhibitor T30177 forms a stacked dimeric G-quadruplex structure containing bulges. *Nucleic Acids Res.*, **39**, 8984–8991.
47. Li,M.H., Zhou,Y.H., Luo,Q. and Li,Z.S. (2010) The 3D stability of G-quadruplexes of HIV-1 integrase inhibitors: molecular dynamics simulation in aqueous solution and in the gas phase. *J. Mol. Model*, **16**, 645–657.
48. Parkinson,G.N., Ghosh,R. and Neidel,S. (2007) Structural bases for binding of porphyrin to human telomers. *Biochemistry*, **46**, 2390–2397.
49. Freyer,M.W., Buscaglia,R., Kaplan,K., Cashman,D., Hurley,L.H. and Lewis,E.A. (2007) Biophysical studies of the c-MYC NHE III1 promoter: model quadruplex interactions with a cationic porphyrin. *Biophys. J.*, **92**, 2007–2015.
50. Goalstone,M., Leitner,J.W. and Draznin,B. (1997) GTP loading of farnesylated p21Ras by insulin at the plasma membrane. *Biochem. Biophys. Res. Commun.*, **239**, 42–45.
51. Ulsh,L.S. and Shih,T.Y. (1984) Metabolic turnover of human c-rasH p21 protein of EJ bladder carcinoma and its normal cellular and viral homologs. *Mol. Cell. Biol.*, **4**, 1647–1652.
52. Zhang,Z., Jiang,G., Yang,F. and Wang,J. (2006) Knockdown of mutant K-ras expression by adenovirus-mediated siRNA inhibits the in vitro and in vivo growth of lung cancer cells. *Cancer Biol. Ther.*, **5**, 1481–1486.
53. Lebedeva,I.V., Su,Z.Z., Emdad,L., Kolomeyer,A., Sarkar,D., Kitada,S., Waxman,S., Reed,J.C. and Fisher,P.B. (2007) Targeting inhibition of K-ras enhances Ad.mda-7-induced growth suppression and apoptosis in mutant K-ras colorectal cancer cells. *Oncogene*, **26**, 733–744.
54. Dausse,E., Da Rocha Gomes,S. and Toulmé,J.J. (2009) Aptamers: a new class of oligonucleotides in the drug discovery pipeline? *Curr. Opin. Pharmacol.*, **9**, 602–607.
55. Mischiati,C., Borgatti,M., Bianchi,N., Rutigliano,C., Tomassetti,M., Feriotto,G. and Gambari,R. (1999) Interaction of the human NF-kappaB p52 transcription factor with DNA-PNA hybrids mimicking the NF-kappaB binding sites of the human immunodeficiency virus type 1 promoter. *J. Biol. Chem.*, **274**, 33114–33122.
56. Bezzerri,V., Borgatti,M., Nicolis,E., Lampronti,I., Dechecchi,M.C., Mancini,I., Rizzotti,P., Gambari,R. and Cabrini,G. (2008) Transcription factor oligodeoxynucleotides to NF-kappaB inhibit transcription of IL-8 in bronchial cells. *Am. J. Respir. Cell Mol. Biol.*, **39**, 86–96.

57. Cabrini,G., Bezzerri,V., Mancini,I., Nicolis,E., Dechecchi,M.C., Tamanini,A., Lampronti,I., Piccagli,L., Bianchi,N., Borgatti,M. *et al*. (2010) Targeting transcription factor activity as a strategy to inhibit pro-inflammatory genes involved in cystic fibrosis: decoy oligonucleotides and low-molecular weight compounds. *Curr. Med. Chem*., **17**, 4392–4404.
58. Crinelli,R., Carloni,E., Menotta,M., Giacomini,E., Bianchi,M., Ambrosi,G., Giorgi,L. and Magnani,M. (2010) Oxidized ultrashort nanotubes as carbon scaffolds for the construction of cell-penetrating NF-kappaB decoy molecules. *ACS Nano*., **4**, 2791–2803.
59. Souissi,I., Najjar,I., Ah-Koon,L., Schischmanoff,P.O., Lesage,D., Le Coquil,S., Roger,C., Dusanter-Fourt,I., Varin-Blank,N., Cao,A. *et al*. (2011) STAT3-decoy oligonucleotide induces cell death in a human colorectal carcinoma cell line by blocking nuclear transfer of STAT3 and STAT3-bound NF-κB. *BMC Cell Biol*., **12**, 12–14.
60. Zhang,X., Zhang,J., Wang,L., Wei,H. and Tian,Z. (2007) Therapeutic effects of STAT3 decoy oligodeoxynucleotide on human lung cancer in xenograft mice. *BMC Cancer*, **7**, 149–160.
61. Sakaguchi,M., Nukui,T., Sonegawa,H., Murata,H., Futami,J., Yamada,H. and Huh,N.H. (2005) Targeted disruption of transcriptional regulatory function of p53 by a novel efficient method for introducing a decoy oligonucleotide into nuclei. *Nucleic Acids Res*., **33**, e88.
62. Tomita,N., Kim,J.Y., Gibbons,G.H., Zhang,L., Kaneda,Y., Stahl,R.A., Ogborn,M., Venderville,B., Morishita,R., Baran,D. *et al*. (2004) Gene therapy with an E2F transcription factor decoy inhibits cell cycle progression in rat anti-Thy 1 glomerulonephritis. *Int. J. Mol. Med*., **13**, 629–636.
63. Tomita,T., Kunugiza,Y., Tomita,N., Takano,H., Morishita,R., Kaneda,Y. and Yoshikawa,H. (2006) E2F decoy oligodeoxynucleotide ameliorates cartilage invasion by infiltrating synovium derived from rheumatoid arthritis. *Int. J. Mol. Med*., **18**, 257–265.
64. Cho,J.W., Cha,Y.C. and Lee,K.S. (2008) AP-1 transcription factor decoy reduces the TGF-beta1-induced cell growth in scleroderma fibroblasts through inhibition of cyclin E. *Oncol. Rep*., **19**, 737–741.
65. Choi,E.W., Nayak,L.V. and Bates,P.J. (2010) Cancer-selective antiproliferative activity is a general property of some G-rich oligodeoxynucleotides. *Nucleic Acids Res*., **38**, 1623–1635.
66. Bates,P.J., Choi,E.W. and Nayak,L.V. (2009) G-rich oligonucleotides for cancer treatment. *Methods Mol. Biol*., **542**, 379–392.
67. McMicken,H.W., Bates,P.J. and Chen,Y. (2003) Antiproliferative activity of G-quartet-containing oligonucleotides generated by a novel single-stranded DNA expression system. *Cancer Gene Ther*., **10**, 867–869.
68. Reyes-Reyes,E.M., Teng,Y. and Bates,P.J. (2010) A new paradigm for aptamer therapeutic AS1411 action: uptake by macropinocytosis and its stimulation by a nucleolin-dependent mechanism. *Cancer Res*., **70**, 8617–8629.
69. Bossone,S.A., Asselin,C., Patel,A.J. and Marcu,K.B. (1992) MAZ, a zinc finger protein, binds to c-MYC and C2 gene sequences regulating transcriptional initiation and termination. *Proc. Natl Acad. Sci. USA*, **89**, 7452–7466.
70. Song,J., Murakami,H., Tsutsui,H., Tang,X., Matsumura,M., Itakura,K., Kanazawa,I., Sun,K. and Yokoyama,K.K. (1998) Genomic organization and expression of a human gene for Myc-associated zinc finger protein (MAZ). *J. Biol. Chem*., **273**, 20603–20614.
71. Parks,C.L. and Shenk,T. (1997) Activation of the adenovirus major late promoter by transcription factors MAZ and Sp1. *J. Virol*., **71**, 9600–9607.
72. Leroy,C., Manen,D., Rizzoli,R., Lombès,M. and Silve,C. (2004) Functional importance of Myc-associated zinc finger protein for the human parathyroid hormone (PTH)/PTH-related peptide receptor-1 P2 promoter constitutive activity. *J. Mol. Endocrinol*., **32**, 99–113.
73. Song,H., Claycomb,R., Tai,T.C. and Wong,D.L. (2003) Regulation of the Rat phenylethanolamine N-methyltransferase gene by transcription factors Sp1 and MAZ. *Mol. Pharmacol*., **64**, 1180–1188.
74. Himeda,C.L., Ranish,J.A. and Hauschka,S.D. (2008) Quantitative proteomic identification of MAZ as a transcriptional regulator of muscle-specific genes in skeletal and cardiac myocytes. *Mol. Cell Biol*., **28**, 6521–3655.
75. Schneider,U.V., Géci,I., Jøhnk,N., Mikkelsen,N.D., Pedersen,E.B. and Lisby,G. (2011) Increasing the analytical sensitivity by oligonucleotides modified with para- and ortho-twisted intercalating nucleic acids—TINA. *PLoS One*, **6**, e20565.
76. Ellis,C.A. and Clark,G. (2000) The importance of being K-ras. *Cell Signal*, **12**, 425–434.
77. Zhang,Y., Nemunaitis,J., Samuel,S.K., Chen,P. and Shen,Y. (2006) Antitumor activity of an oncolytic adenovirus-delivered oncogene small interference RNA. *Cancer Res*., **66**, 9736–9743.
78. Cogoi,S., Quadrifoglio,F. and Xodo,L.E. (2004) G-rich oligonucleotide inhibits the binding of a nuclear protein to the Ki-ras promoter and strongly reduces cell growth in human carcinoma pancreatic cells. *Biochemistry*, **43**, 2512–2523.